High resolution x-ray transition-edge sensor cooled by tunnel junction refrigerators

N. A. Miller,[a] G. C. O'Neil, J. A. Beall, G. C. Hilton, K. D. Irwin, D. R. Schmidt, L. R. Vale, and J. N. Ullom
National Institute of Standards and Technology, Boulder, Colorado 80305, USA

(Received 17 March 2008; accepted 2 April 2008; published online 21 April 2008)

We demonstrate cooling of an x-ray transition-edge sensor (TES) using solid-state refrigerators based on normal-metal/insulator/superconductor (NIS) tunnel junctions. We are able to operate the NIS refrigerators at a starting temperature of 260 mK, which is 75 mK above the TES transition temperature (185 mK), and still achieve high quality x-ray spectra with an energy resolution of 9.5 ± 0.3 eV full width at half maximum at 5.9 keV. The maximum cooling achieved by the NIS refrigerators is 110 mK, from a starting temperature of 300 down to 190 mK. © *2008 American Institute of Physics*. [DOI: 10.1063/1.2913160]

Normal-metal/insulator/superconductor (NIS) tunnel junctions can be used as solid-state refrigerators with the potential to cool from 300 to 100 mK.[1,2] Biasing an NIS junction causes the hottest electrons in the normal metal to tunnel across the insulator barrier into the superconductor, which cools the remaining normal-metal electrons. Extending the normal metal onto a membrane as a cold finger cools both the electrons and lattice of the electrically separate membrane.[3,4] In previous work, we dramatically increased the size and cooling power of NIS junctions.[5,6] Here, we demonstrate the successful integration of NIS refrigerators with a separate, technologically useful payload.

The payload is a superconducting transition-edge sensor (TES) designed for x-ray detection. TESs are a critical technology for high-resolution x-ray spectroscopy, especially for applications in materials analysis and astronomy.[7,8] X-ray TESs are superconducting thin films typically operated near 100 mK for optimal performance. Traditional refrigerators used to reach 100 mK, adiabatic demagnetization refrigerators (ADRs) and dilution refrigerators, have drawbacks for some applications due to their complexity and size. Examples include commercial x-ray microanalysis systems and space-borne detectors. Combining NIS refrigerators with a sorption-pumped ^{3}He system (base temperature 260 mK), which is relatively inexpensive and small, provides a third option for cooling devices to 100 mK. Alternatively, combining NIS refrigerators with an ADR allows for more design options, including extended hold times, reduced mass, and lower stray magnetic fields from the ADR.

An x-ray TES with integrated NIS refrigerators is shown in Fig. 1(a). The TES is suspended on a 500 nm thick low-stress SiN_x membrane that is connected to the substrate through four 39 μm wide by 23 μm long corner legs and one 33 μm wide by 110 μm long side leg. The TES is a 250 μm by 250 μm bilayer of Mo and Cu, with a critical temperature $T_c = 185$ mK and a normal-state resistance $R_{n,\mathrm{TES}} = 16.2$ mΩ. Three normal-metal Cu bars are added to control the transition width and noise characteristics.[9] A bismuth absorber (not shown), 1.55 μm thick, is deposited over the TES to increase x-ray absorption. The TES is voltage biased with a shunt resistor $R_{\mathrm{sh}} = 727$ $\mu\Omega$ and readout by two stages of superconducting quantum interference devices (SQUIDs). To measure the performance of the TES, an ^{55}Fe x-ray source is used to irradiate the TES through a 250 μm diameter collimator.

A pair of NIS refrigerator junctions, each 15 μm wide by 25 μm long, is located on the bulk substrate at each corner of the membrane [Fig. 1(b)]. The normal-metal electrodes of the junctions are Al doped with Mn to suppress superconductivity and the superconducting electrodes are elemental Al. The eight junctions in series have a normal-state resistance $R_{n,\mathrm{NIS}} = 36$ Ω and zero-bias leakage resistance $R_{\mathrm{lk}} \sim 540$ $k\Omega$. The normal metal of each junction pair extends onto the membrane as a cold finger. An additional layer of Cu is added to the cold fingers to increase the thermal conductivity.[4]

Completed devices are cooled in an ADR, allowing NIS and TES behavior to be characterized down to an ADR temperature T_{ADR} of 50 mK.

Johnson noise thermometry (JNT) is used to measure the temperature of the unbiased TES without dissipating any power. A Helmholtz coil outside the dewar is used to apply a perpendicular magnetic field of 440 μT, which suppresses the TES T_c from 185 to below 50 mK, making it possible to use JNT at all ADR temperatures. The magnetic field has only a small effect on the NIS *I-V* curves and does not significantly change the cooling performance. The current noise

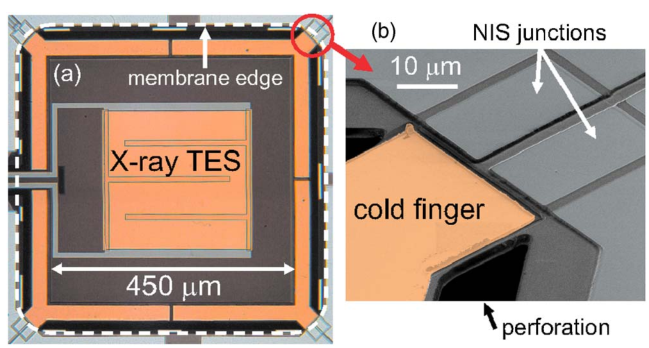

FIG. 1. (Color online) (a) TES x-ray sensor integrated with NIS refrigerators (Bi absorber not shown). Four pairs of NIS refrigerators are located at the corners of a SiN_x membrane (dashed outline). Y-shaped cold fingers extend from the normal metal of the NIS junctions onto the membrane. (b) False-color SEM image of membrane corner.

[a]Electronic mail: nmiller@boulder.nist.gov.

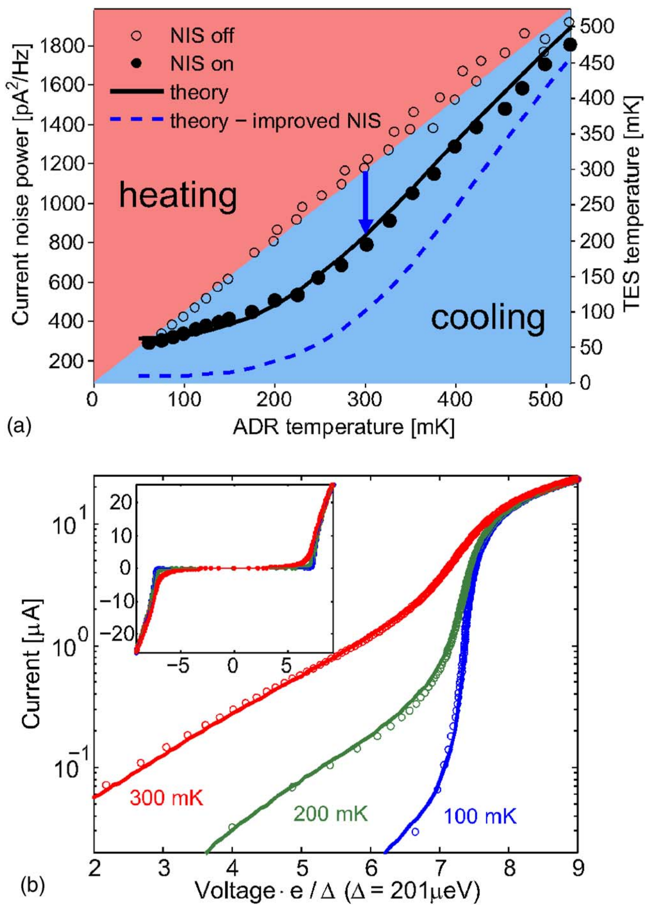

FIG. 2. (Color online) (a) JNT of the unbiased TES with NIS refrigerators off (open circles) and on (solid circles). Noise power averaged between 0.6 and 2 kHz (left axis) and cooling calculated from Eq. (2) (right axis). The NIS cooling is well matched by theory (solid line). Potential cooling with improved NIS refrigerators shown as dashed line. (b) Log-current plot of NIS *I*-*V* curves. Data (circles) and theory (lines) show excellent agreement. The inset shows the *I*-*V*s on a linear current scale (axes units unchanged).

power (I_N^2) of the TES when the NIS refrigerators are off is

$$I_{N,\mathrm{off}}^2 = \frac{4k_B}{(R_{n,\mathrm{TES}} + R_{\mathrm{sh}})} T_{\mathrm{ADR}} + I_{N,\mathrm{sys}}^2, \tag{1}$$

where $I_{N,\mathrm{sys}}$ is the system current noise ($6\ \mathrm{pA}/\sqrt{\mathrm{Hz}}$) due to the SQUIDs and k_B is the Boltzmann constant. Biasing the NIS refrigerators reduces the temperature of the cold fingers and the TES (T_{TES}). The reduced current noise power is

$$I_{N,\mathrm{on}}^2 = \frac{4k_B R_{n,\mathrm{TES}}}{(R_{n,\mathrm{TES}} + R_{\mathrm{sh}})^2} T_{\mathrm{TES}} + \frac{4k_B R_{\mathrm{sh}}}{(R_{n,\mathrm{TES}} + R_{\mathrm{sh}})^2} T_{\mathrm{ADR}} + I_{N,\mathrm{sys}}^2, \tag{2}$$

which can be solved for T_{TES} to find the temperature reduction [Fig. 2(a)]. Maximum cooling is observed from an ADR temperature of 300 mK to a reduced TES temperature of 190 mK. The use of JNT allows unambiguous thermometry even at the lowest temperatures. For instance, we observe cooling from 60 to 54 mK and from 75 to 59 mK.

To calculate the theoretical cooling shown in Fig. 2(a), we use an NIS thermal model to predict the temperature reduction of the normal metal as a function of bias voltage and bath temperature.[5] We fit the measured NIS *I*-*V* curves [Fig. 2(b)] to determine two model parameters: $\Delta = 201\ \mu$eV is the superconducting energy gap of the Al and

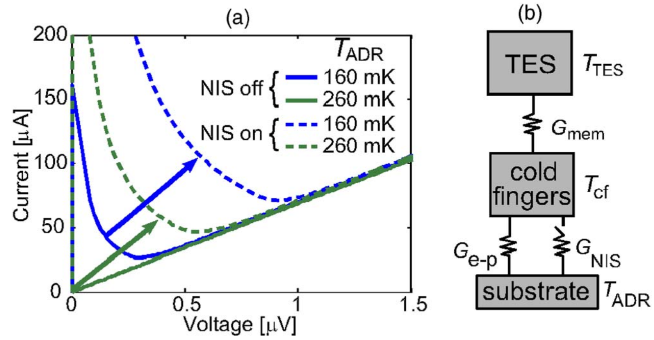

FIG. 3. (Color online) (a) TES *I*-*V*s with the NIS refrigerators off (solid lines) and on (dashed lines). (b) Thermal model for NIS-cooled TES. Thermal conductances *G* and temperatures *T* are labeled for each element.

$\beta = 9\%$ is the percentage of the power deposited in the superconductor that returns to the normal metal. The close agreement between the *I*-*V* data and fits, over three decades of current and numerous bath temperatures, lends authority to the temperature predictions of the model. Potential cooling with improved NIS refrigerators is also shown in Fig. 2(a), where we have assumed more transparent tunnel junctions and no power return ($\beta = 0$). This curve shows that NIS refrigerators have the potential to provide working temperatures below 100 mK from starting temperatures near 300 mK. We have previously fabricated devices with more transparent tunnel junctions and a reduced power return ($\beta = 4\%$).[5] A further reduction in β is attainable by improvements in the design of the quasiparticle traps, which trap and thermalize power deposited in the superconductor.[10]

With the NIS refrigerators on, we are able to operate the TES at ADR temperatures above T_c by cooling the cold fingers below T_c. When the TES is biased and dissipating power, the TES *I*-*V* curves [Fig. 3(a)], combined with a separate measurement of the thermal conductance of the membrane G_{mem} [Fig. 3(b)], can be used to determine the cooling provided by the NIS refrigerators when under load. TES *I*-*V* curves alone are insufficient because biasing the NIS refrigerators increases the total thermal conductance between the TES and the substrate.[11] We have directly measured G_{mem} in a separate test device where the cold fingers and NIS junctions were replaced by a Cu film that extended onto the substrate around the full perimeter of the TES. At a TES bias power of 22 pW, the NIS refrigerators reduce the effective bath temperature of the TES from 260 to 162 mK. Hence, the 22 pW load from the biased TES reduces the cooling by 7 mK from the unbiased case in Fig. 2(a).

Figure 4(a) shows an NIS-cooled TES x-ray spectrum taken at an ADR temperature of 260 mK, which is 75 mK above the TES T_c. A theoretical fit to the Mn $K\alpha$ complex yields an energy resolution of 9.5 ± 0.3 eV full width at half maximum (FWHM) at 5.9 keV.[12] This resolution is an improvement over previous work using superconducting detectors at cryostat temperatures above 200 mK.[13] As a further comparison, current microanalysis systems employ Si-based detectors with an energy resolution of 130 eV at 5.9 keV, which is insufficient to resolve many technologically important x-ray lines.[7] Our present resolution of 9.5 eV is by no means the physical limit. We calculate that the resolution can be improved to 5 eV by reducing the size of the TES and halving the steepness of the superconducting transition. Improvements in NIS cooling performance [Fig. 2(a)] will al-

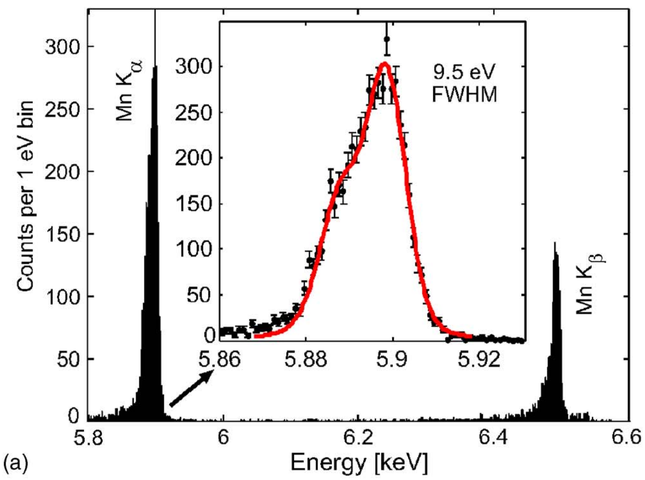

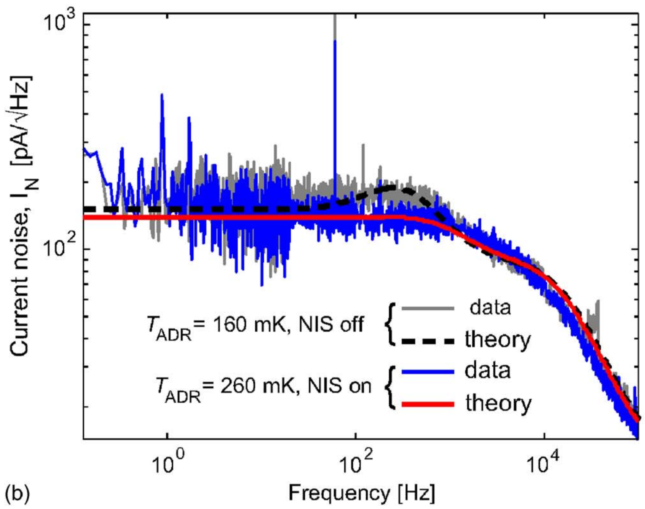

FIG. 4. (Color online) (a) x-ray spectrum (9069 pulses) at an ADR temperature of 260 mK. The inset shows a zoomed view of the 5.9 keV Mn $K\alpha$ complex and the theoretical fit. The TES is biased at 60% $R_{n,\mathrm{TES}}$ with a bias power of 22 pW and a fall time of 160 μs. (b) TES current noise with the NIS refrigerators off and on. The TES is biased at 40% $R_{n,\mathrm{TES}}$. ADR temperatures were chosen to compare the same TES bath temperature.

low for a lower T_c of 120 mK and a calculated resolution below 2.5 eV at 5.9 keV.

The NIS refrigerators do not degrade the noise performance of the TES. The measured current noise of the TES is shown in Fig. 4(b) with the NIS refrigerators off and on. The noise theory curves are based on the two-body thermal model in Fig. 3(b), where we have used measured and calculated thermal conductance values, complex impedance fits to obtain the heat capacities and derivatives of the TES resistance, and a current noise fit to obtain the excess noise parameter.[14–16] We have also measured the long-term stability (6 h) of the x-ray pulse heights and saw no difference with the NIS refrigerators either off or on.

In conclusion, we have used JNT to measure NIS cooling down to starting temperatures of 60 mK, achieving a maximum reduction of 110 mK from an ADR temperature of 300 mK. We have demonstrated successful cooling of a high-resolution x-ray TES using NIS refrigerators, allowing the TES to be operated at ADR temperatures above T_c. We have achieved an energy resolution of 9.5 ± 0.3eV (FWHM) at 5.9 keV at an ADR temperature of 260 mK (75 mK above the TES T_c). The use of integrated NIS refrigerators makes the remarkable performance of modern cryogenic sensors available from 300 mK platforms.

This work was supported by the NIST Office of Microelectronics Programs and the NASA ROSES program under Grant No. APRA04-0037-0178.

[1] M. Nahum, T. M. Eiles, and J. M. Martinis, Appl. Phys. Lett. **65**, 3123 (1994).
[2] M. M. Leivo, J. P. Pekola, and D. V. Averin, Appl. Phys. Lett. **68**, 1996 (1996).
[3] A. J. Manninen, M. M. Leivo, and J. P. Pekola, Appl. Phys. Lett. **70**, 1885 (1997).
[4] N. A. Miller, A. M. Clark, A. Williams, S. T. Ruggiero, G. C. Hilton, J. A. Beall, K. D. Irwin, L. R. Vale, and J. N. Ullom, IEEE Trans. Appl. Supercond. **15**, 556 (2005).
[5] A. M. Clark, A. Williams, S. T. Ruggiero, M. L. van den Berg, and J. N. Ullom, Appl. Phys. Lett. **84**, 625 (2004).
[6] A. M. Clark, N. A. Miller, A. Williams, S. T. Ruggiero, G. C. Hilton, L. R. Vale, J. A. Beall, K. D. Irwin, and J. N. Ullom, Appl. Phys. Lett. **86**, 173508 (2005).
[7] D. A. Wollman, K. D. Irwin, G. C. Hilton, L. L. Dulcie, D. E. Newbury, and J. M. Martinis, J. Microsc. **188**, 196 (1997).
[8] F. S. Porter, Nucl. Instrum. Methods Phys. Res. A **520**, 354 (2004).
[9] J. N. Ullom, W. B. Doriese, G. C. Hilton, J. A. Beall, S. Deiker, W. D. Duncan, L. Ferreira, K. D. Irwin, C. D. Reintsema, and L. R. Vale, Appl. Phys. Lett. **84**, 4206 (2004).
[10] J. N. Ullom, P. A. Fisher, and M. Nahum, Phys. Rev. B **61**, 14839 (2000).
[11] N. A. Miller, J. A. Beall, G. C. Hilton, K. D. Irwin, G. C. O'Neil, D. R. Schmidt, L. R. Vale, and J. N. Ullom, J. Low Temp. Phys. **150**, 635 (2008).
[12] G. Holzer, M. Fritsch, M. Deutsch, J. Hartwig, and E. Forster, Phys. Rev. A **56**, 4554 (1997).
[13] L. Li, L. Frunzio, C. Wilson, D. E. Prober, A. E. Szymkowiak, and S. H. Moseley, J. Appl. Phys. **90**, 3645 (2001).
[14] K. D. Irwin and G. C. Hilton, *Cryogenic Particle Detection* (Springer, Berlin, Germany, 2005), Vol. 99, pp. 63–149.
[15] M. A. Lindeman, K. A. Barger, D. E. Brandl, S. G. Crowder, L. Rocks, and D. McCammon, Rev. Sci. Instrum. **78**, 043105 (2007).
[16] D. Golubev and L. Kuzmin, J. Appl. Phys. **89**, 6464 (2001).